

# Mechanism and Application of Photocatalytic Hydrogen Generation by Cobalt Oximes

Shuai Zhang<sup>a</sup>, Lei Chen<sup>\*, b</sup>

<sup>a</sup>College of Materials Science and Engineering, Jilin Jian Zhu University, Changchun 130118, China

<sup>b</sup>College of municipal and environmental engineering, Jilin Jian Zhu University, Changchun 130118, China  
[chenlei@jju.edu.cn](mailto:chenlei@jju.edu.cn)

In this work, cobaloxime molecules have been synthesized in our group, and new photoinduced hydrogen production systems have been constructed. Based on the new systems for hydrogen production, the mechanism of electron transfer as well as system degradation have been investigated in detail. According to the simulation results in Gaussian 03 software, we implement the ideal catalytic process for hydrogen production induced by cobaloxime. In cobaloxime molecular, Co is indeed the catalytic center, that is to say, it is the change of electrovalence of Co atoms from 3 to 2 and 1, and then from 1 to 3, implies the catalytic process. Through the simulation, we can obtain the middle products in the catalytic process clearly. Moreover, the electron charge of middle products can be analyzed, based on which the catalytic pathway predicted by other experimental results is confirmed. All this provides the theoretical basis for the hydrogen production catalyzed by cobaloxime molecular.

## 1. Introduction

How to utilize inexhaustible solar energy to prepare hydrogen from photolysis water efficiently and inexpensively is one of the hotspots in the hydrogen energy development and augurs well for the future development of new energy in our country. Currently, in view of the increasingly shortage of energy resources and the continuously serious environmental pollution, the photocatalytic water splitting for hydrogen production by utilizing the solar energy is an ultimate method to resolve energy and environmental problems (Kudo and Miseki, 2009). In the process of hydrogen production by photocatalytic water splitting, the key challenge for capturing hydrogen by solar energy is how to develop the catalytic material with high photocatalytic activity and hydrogen generation efficiency in the visible light range at a low cost. So far, scholars have made extensive studies on the photocatalytic materials, especially on some photocatalysts about metal oxides and sulfides (Fujishima and Honda, 1972; Bernhard and Allen, 1978; Mark and Mate, 2010; Bigi et al., 2010; Osterloh, 2008) such as TiO<sub>2</sub> and CdS. Although TiO<sub>2</sub> features non-toxicity, low cost, chemical stability and other properties, a larger energy gap makes the TiO<sub>2</sub> only response to the solar ultraviolet light at a low utilization rate; the application of CdS is also limited due to its liable light corrosion.

In this paper, we mainly explore the catalytic hydrogen production cycle of cobalt oximes by computational simulation, and probe into the internal charge transport process to reveal a real process about how the cobalt oxime molecules are catalyzed.

## 2. Model

The [Co(dmgh)<sub>2</sub>pyCl] molecule is taken as a study object in this paper, by which, the charge transport during hydrogen production is simulated using Gaussian03. The cobalt oxime [Co(dmgh)<sub>2</sub>pyCl] molecule geometry model is shown in Figure 1:

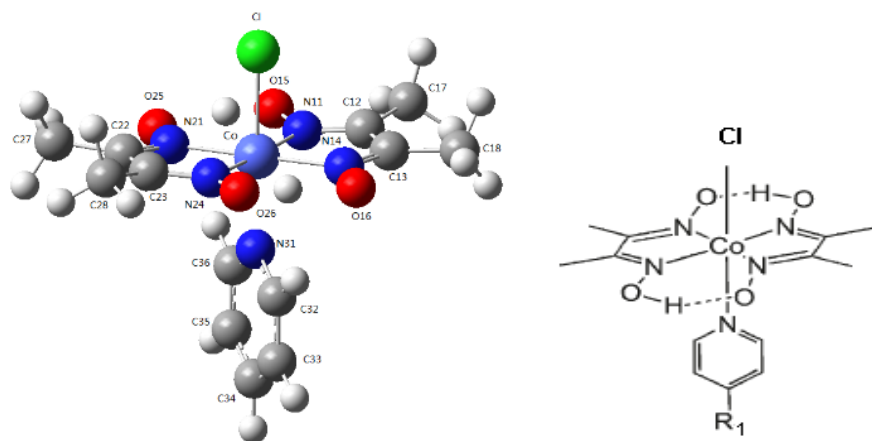


Figure 1: Cobalt oxime [Co(dmgh)2pyCl] molecule geometry model

First, the molecular structure model for cobalt oximes is built on the Gaussian03 G-View interface. Then the [Co (dmgh) 2pyCl] molecular geometry structure is optimized by using the Density Functional Theory (DFT) in Gaussian03 quantum chemistry calculation software. The geometrical parameters of optimized molecule are shown in the Table 1. It is obvious that the results of the DFT computational simulation coincide with those from other scholars' experiments, which demonstrates the rationalities of the simulation and the preferences as a reasonable parameter setting for further charge transfer computations.

Table 1: The geometrical parameters of optimized molecule

Bond length(Å)/angle (°)	DFT computation	Data from literature	Bond length(Å)/angle (°)	DFT computation	Data from literature
Co1-C1	1.94889	1.931(3)	N11-Co1-N21	98.51726	98.59(13)
Co1-N11	1.91883	1.883(2)	N14-Co1-N24	98.57008	98.19(12)
Co1-N14	1.92780	1.891(2)	N11-Co1-N14	81.43517	81.77(12)
Co1-N21	1.92683	1.889(2)	N21-Co1-N24	81.42611	81.42(13)
Co1-N24	1.92024	1.885(2)	N11-Co1-C1	86.68097	89.91(17)
Co1-N31	2.05502	2.040(2)	N11-Co1-N31	91.32890	90.75(12)
N11-O15	1.36514	1.358(3)	N14-Co1-C1	91.49525	87.75(10)
N24-O26	1.36485	1.353(3)	N14-Co1-N31	90.46430	89.10(9)
N14-O16	1.30531	1.322(3)	N21-Co1-C1	87.59563	91.60(11)
N21-O25	1.30455	1.337(4)	N21-Co1-N31	90.44449	91.55(8)
N11-Co1-N24	176.79654	177.16(10)	N24-Co1-C1	90.11695	87.26(17)
N14-Co1-N21	179.09083	179.25(12)	N24-Co1-N31	91.87438	92.09(12)

The energy of geometrically optimized [Co (dmgh) 2pyCl] molecule is then improved using DFT. By calculating the energy level and distribution at the LUMO orbit, we discovery that the LUMO of [Co (dmgh) 2pyCl] molecule lies in the axial pyridyl group, as shown in Figure. 2:

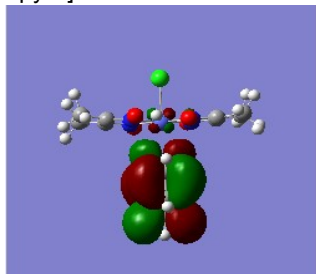


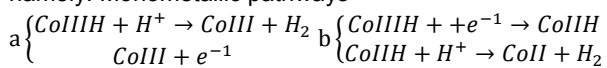
Figure 2: LUMO of [Co (dmgh) 2pyCl] molecule lies in the axial pyridyl group

The result from this calculation shows that the cobalt oxime molecule [Co (dmgh) 2pyCl] accesses to the catalytic center from axial orbit when it receives electrons generated after the sunlight is absorbed by the sensitizer.

Under the condition that the axial ligand is known as the means for [Co(dmgh)2pyCl] molecule to receive the electrons, we have tuned the axial ligands of the central Co, mainly including the ligand species on the pyridyl group. It is found that when the ligand groups on pyridine -CH<sub>3</sub>, -CH<sub>2</sub>CH<sub>3</sub>, -OH, -CN and -N (CH<sub>3</sub>) 2 respectively take place of the opposite group of N on the pyridine ligand that links to Co, the LUMO orbit energy level remains on the pyridyl group. In this type of axial ligand cobalt oxime molecule, the electrons enter the catalytic center only from the axial ligand.

In the current studies on the photocatalytic water splitting system, the principal concerns are how to improve the utilizations of visible light in the sunlight, the rate of hydrogen production and the quantum yield. The scholars still resort to the experimental approaches in this field (Young et al., 1975; Esswein and Nocera, 2007; Sun et al., 2001). A catalysis in homogenous system is built with different catalyst molecular structures compatible with different photosensitizers, sacrificial agents and solutions, as developed, to probe into the law of quantum yield. The most efficient catalytic hydrogen production system reported in the literature is: [Co (dmgh) 2pyCl] as a catalyst, Pt (ttpy) (C≡CPh) ClO<sub>4</sub> as a dye and triethanolamine TEOA (0.27 M) as a cytoplasm. After an irradiation of 10 hours at λ > 410 nm, the catalytic hydrogen production can reach up to about 2150 cycles. However, the lack of theoretical study on the charge transport path and its mechanism in catalytic hydrogen production badly restricts the hydrogen production efficiency. In many experiments, it is proposed that the catalytic hydrogen production cycle of cobalt oxime molecules is a process related to the change of the Co charge. The change of the cobalt price level measured by the cyclic voltammetry is based on to predict the results of hydrogen production by catalytic cobalt oximes. For the mechanism of photocatalytic hydrogen production by cobalt oximes, most of the studies resort to the cyclic voltammetry to predict the catalytic hydrogen production path based on the change of metal cobalt price level in the ligand center. In the process of hydrogen reaction, Cobalt Co(III) ligands, in turn, generate divalent and monovalent cobalt Co(II) and Co(I) midbodies by the reduction of two single electrons, where the Co(I) midbody is a key intermediate product in the hydrogen production process. A nucleophilic Co(I) midbody interacts with protons to form hydride Co(III)H, namely: Co(III) + e<sup>-</sup> → Co(II); Co(II) + e<sup>-</sup> → Co(I); Co(I) + H<sup>+</sup> → Co(III)H

Subsequently, the path for catalytic hydrogen production is not unique. Currently, there are two hydrogen production mechanisms available by everyone, i.e. monometallic and bimetallic mechanisms. In the first place, Co (III) hydride can produce hydrogen and a Co (III) by further proton addition, or Co (III) hydride is further restored to Co (II) and produce Hydrogen and one Co (II) by proton addition, so that the monometallic catalysis mechanism is achieved; the other path is that hydrogen and two Co (II) are produced by the reaction of two Co (III) hydrides. Although the latter path seems to be fully feasible in chemical experiments, it is more difficult to work out the computational simulation and get experimentally relevant information. In the study, we mainly use the computational simulation to simulate and calculate the catalytic mechanism of the monometal in order to obtain a series of physical information about midbodies in the process of catalytic hydrogen production. However, these intermediate products are hardly found and recorded in the lab. In the monometallic catalyst path, the hydride Co(III)H charged hydrogen production process also has two ways, namely: Monometallic pathways



Based on the monometallic catalysis, this study uses Gaussian computational simulation to simulate the transport path of the charge, as shown below:

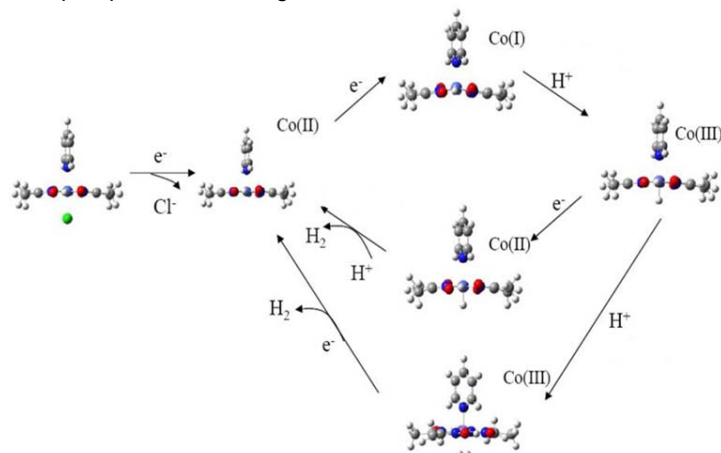


Figure 3: Schematic diagram of computational simulation

### 3. Discussion

The catalytic cycle diagram is the result of a simulation. As can be seen from the figure, the trivalent  $\text{CoIII}$  complex absorbs photo-induced electrons and becomes a bivalent  $\text{CoII}$ . At this time, the axial ligand  $\text{Cl}$  group breaks away from the catalyst center and the divalent  $\text{CoII}$  complex enters the true process of catalytic cycle. As shown in the figure, when the catalytic cycle is ended,  $\text{CoII}$  complex is returned; the divalent  $\text{CoII}$  complex continues to absorb electrons and convert into the monovalent  $\text{CoI}$  complex which is also obviously nucleophilic to absorb protons, generating trivalent hydride  $\text{CoIIH}$  as a key intermediate product in catalytic hydrogen production, and difficult to be observed in the lab but clearly visible about its physical properties in the simulation; then the  $\text{CoIIH}$  hydride continues to react with protons or electrons. This reaction depends on the acidic conditions of the photocatalysis system. When the acidity is strong,  $\text{CoIIH}$  hydride reacts with the protons to generate  $\text{CoIII}$  ( $\text{H}_2$ ). In fact, hydrogen has been generated now. When  $\text{H}_2$  is far away from the catalytic center  $\text{Co}$  by a distance of 5 Å, the energy change is negligible and the trivalent  $\text{CoIII}$  complex continues to absorb electrons to generate divalent  $\text{CoII}$  ones. Now a cycle is ended. When the alkaline in the environmental system is strong,  $\text{CoIIH}$  hydride interacts with the electrons to generate a divalent  $\text{CoIIH}$  hydride which then reacts with the electrons to get hydrogen and divalent  $\text{CoII}$  complexes. Till now, a hydrogen production cycle is over.

In the process of the hydrogen production simulation cycle, it is found that the reason why the charge transfer is impacted lies in the capacities of each intermediate product to absorb and donate electrons. In order to validate the above charge transport process, the physical properties of each intermediate product, mainly the LUMO and HOMO orbit distributions, are analyzed for the reasons that the energy level of the LUMO orbits partly explain the capacity to absorb the electrons, whereas that of the HOMO orbit shows its capacity to donate electrons. Therefore, we analyze the charge transfer process step by step as follows:

Cobalt oxime molecules first absorb light-induced electrons and turn from trivalent  $\text{Co}$  into divalent  $\text{Co}$ . In the distributions of the calculated HOMO and LUMO orbital energy levels, the LUMO orbit concentrates all of them onto the pyridine ligands, and the HOMO orbit distribution changes obviously from the lateral ligands on the trivalent  $\text{Co}$  to the axial ones on the divalent  $\text{Co}$  predominantly on the  $\text{Cl}$  groups. Further analysis of the HOMO orbit distribution on the  $\text{Cl}$  group shows that there is almost no common electron owned by the  $\text{Cl}$  group and the  $\text{Co}$  center, that is to say, the interaction between both is relatively low, which implies that in the process that  $\text{Co}$  group converts from trivalent  $\text{Co}$  to divalent one, the  $\text{Cl}$  group detaches from the cobalt oxime molecule. While the distance between  $\text{Cl}$  and  $\text{Co}$  atoms increases from 2.2545Å in trivalent  $\text{CoIII}$  complex to 2.5588Å in divalent  $\text{CoII}$  complex, which further interprets that there is a weak interaction between the  $\text{Cl}$  group and the  $\text{Co}$  catalytic center. The fact that  $\text{Cl}$  group detaches from the divalent  $\text{CoII}$  complex is further proved.

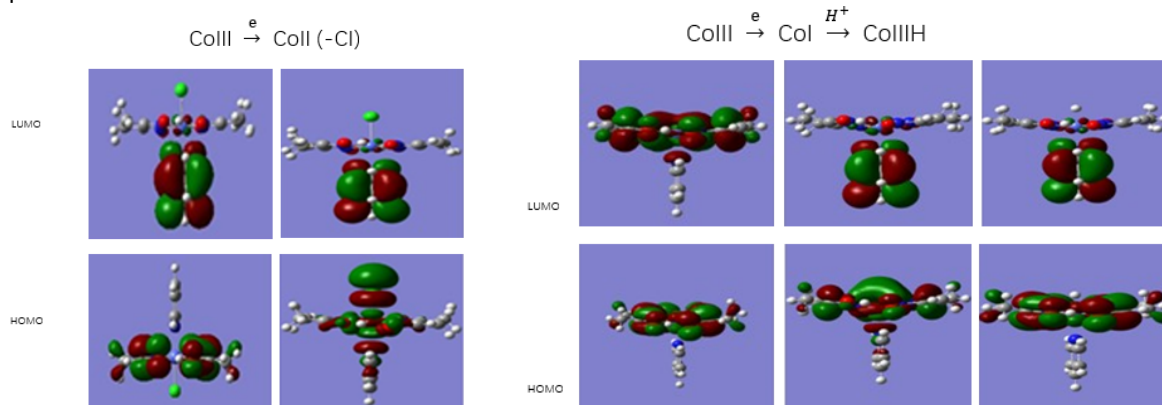


Figure 4:  $\text{CoIII} (+e) \rightarrow \text{CoII}$

Figure 5:  $\text{CoII} (+e) \rightarrow \text{CoI} (+\text{H}^+) \rightarrow \text{CoIIH}$

In this process, we can clearly know about how the HOMO orbit energy distribution changes. The HOMO orbit where the monovalent  $\text{CoI}$  complex is generated from the divalent  $\text{CoII}$  by absorbing electrons mainly distributes the energy on the catalytic center  $\text{Co}$ , which provides conditions for the next proton absorption. It follows that the bond of proton with cobalt oxime molecule must be the linkage between  $\text{H}^+$  and  $\text{Co}$ , and the interatomic distance between  $\text{Co}$  and  $\text{H}$  in the  $\text{CoIIH}$  complex is only 1.497 Å. The fact that hydride  $\text{CoIIH}$  is generated is therefore further confirmed. This is to demonstrate the  $\text{H}_2$  production process simply achieved from the interatomic distance. When the hydride  $\text{CoIIH}$  interacts with the proton, it is found that the distances of catalytic center  $\text{Co}$  from two  $\text{H}$  atoms all equal to 1.8314 Å, significantly higher than 1.497Å between both in

the trivalent hydride  $\text{CoIIIH}$ , which indicates that the interaction between Co and H is weaker, and the distance between two H atoms in the product as generated is 0.7719 Å, very close to the interatomic distance in hydrogen. We can therefore believe that hydrogen has been produced in this process with available trivalent  $\text{CoIII}$  complexes.

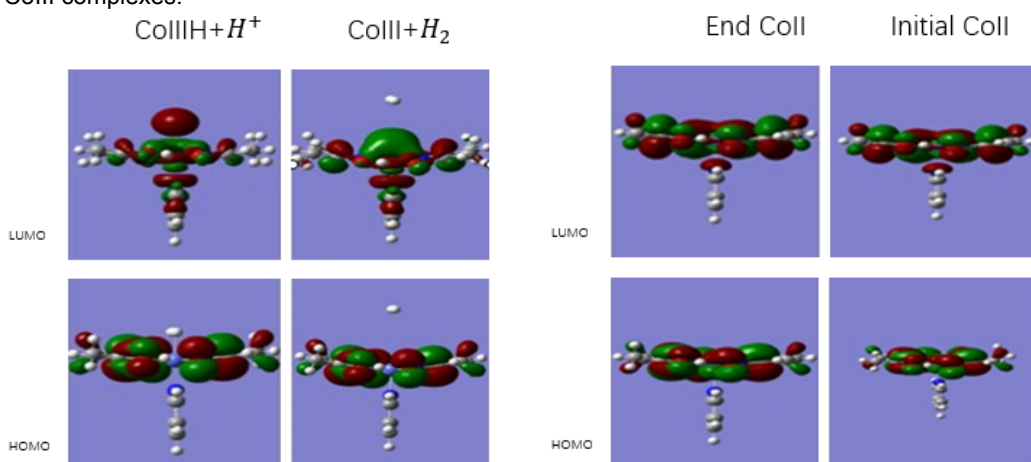


Figure 6:  $\text{CoIIIH} (+\text{H}^+) \rightarrow \text{CoIII} + \text{H}_2$

Figure 7:  $\text{CoIII} (+\text{e}) \rightarrow \text{CoII}$

This is the last step to close the cycle. Now the resultant divalent  $\text{CoII}$  complex should be equivalent to the initial divalent  $\text{CoII}$  complex. The geometric structures of the divalent Co complexes at the start and at the end of the catalytic cycles are therefore compared in order to verify the closure of a catalytic hydrogen production cycle. For the corresponding  $\text{CoII}$  complexes at the start and at the end of catalytic cycles, the geometric structures of the two are shown in Table 2. It can be seen from the table that there is a little difference between the combined constructions of initial and last  $\text{CoII}$  complexes.

Table 2: The geometric structures of the corresponding  $\text{CoII}$  complexes at the start and at the end of catalytic cycles

Bond length(Å)/angle (°)	$\text{CoII}(\text{last})$	$\text{CoII}(\text{initial})$
Co-N11	1.92521	1.92538
Co-N14	1.92590	1.92576
Co-N21	1.92590	1.92577
Co-N24	1.92522	1.92537
Co1-N31	2.14727	2.1478
N11-O15	1.36892	1.36888
N24-O26	1.36892	1.36888
N14-O16	1.30798	1.30802
N21-O25	1.30798	1.30802
N11-Co-N24	167.14820	167.1614
N14-Co-N21	173.88093	173.8770
N11-Co-N21	97.63440	97.63807
N14-Co1-N24	97.63418	97.63661
N11-Co1-N14	81.67445	81.67181
N21-Co1-N24	81.67455	81.67161
N11-Co-N31	96.42585	96.4198
N14-Co-N31	93.05958	93.06174
N21-Co-N31	93.05958	93.06123
N24-Co-N31	96.42595	96.41878

#### 4. Conclusion

In this paper, the relevant intermediate products can be clearly captured by the computational simulation in cyclic process of cobalt oxime catalysis, and the inherent relationship between the electron-absorbing and electron-donating capacities and its catalytic mechanism are grasped as the basis for further recognizing the difference of catalytic hydrogen production cycles by different structures of cobalt oxime molecules and the

theoretical basis for the dependence of the hydrogen production efficiency on the catalyst molecular structure. Using increasingly improved computational simulation technique, and on several fronts such as the impacts of the electronic properties of the coordination group on the electron-absorbing capacity of the catalyst molecules, and the stability of coordination group in the hydrogen production process and its impact on the electronic properties of intermediate products, we can fully understand how important the mechanism the ligand structure acts on the charge transfer rate in the hydrogen production process is as a theoretical basis, which not only provides a theoretical guidance for the design of highly efficient photocatalyst materials, but also helps understand theoretically the dependence of quantum yield on the experimental conditions.

## References

- Bernhard K., Allen J.B., 1978, Heterogeneous photocatalytic decomposition of saturated carboxylic acids on titanium dioxide powder. Decarboxylative route to alkanes, *Journal of the American Chemical Society*, 100(19), 5985-5992, DOI: 10.1021/ja00487a001.
- Bigi J.P., Hanna T.E., Harman W.H., 2010, Electrocatalytic reduction of protons to hydrogen by a water-compatible cobalt polypyridyl platform, *Chemical Communications*, 46(6), 958-960, DOI: 10.1039/b915846d.
- Esswein A.J., Nocera D.G., 2007, Hydrogen production by molecular photocatalysis, *Chemical Reviews*, 107, 4022-4047, DOI: 10.1016/B978-0-12-409547-2.13795-3.
- Fujishima A., Honda K., 1972, Electrochemical Photolysis of water at a semiconductor electrode, *Nature*, 238(5358), 37-40, DOI: 10.1038/238037a0.
- Kudo A., Miseki Y., 2009, Heterogeneous photocatalyst materials for water splitting, *Chemical Society Reviews*, 38, 253-255, DOI: 10.1039/b800489g.
- Mark K., Mate H., 2010, Heterogeneous photocatalytic cleavage of water, *Journal of Materials Chemistry*, 20(4), 627-629, DOI: 10.1039/B910180B.
- Osterloh F.E., 2008, Inorganic Materials as Catalysts for Photochemical Splitting of Water, *Chemistry of Materials*, 20(1), 35-54, DOI: 10.1021/cm7024203.
- Sun L.C., Hammarstroem L., Aakermark B., Styring S., 2001, Towards artificial photosynthesis: ruthenium-manganese chemistry for energy production, *Chemical Society Reviews*, 30(47), 36-49, DOI: 10.1039/A801490F.
- Young R.C., Meyer T.J., Whitten D.G., 1975, Kinetic relaxation measurement of rapid electron transfer reactions by flash photolysis. The conversion of light energy into chemical energy using the Ru(bpy)<sub>3</sub><sup>3+</sup>-Ru(bpy)<sub>3</sub><sup>2+</sup> couple, *Journal of the American Chemical Society*, 97(16), 4781-4782, DOI: 10.1002/chin.197542426